

Electronic Supplementary Information

High thermoelectric performance of Ag doped SnTe polycrystalline bulks via the synergistic manipulation of electrical and thermal transport

Lanling Zhao^{a, b}, Jun Wang^c, Jichao Li^a, Jian Liu^a, Chunlei Wang^{a, *}, Jiyang Wang^d and Xiaolin Wang^{b, *}

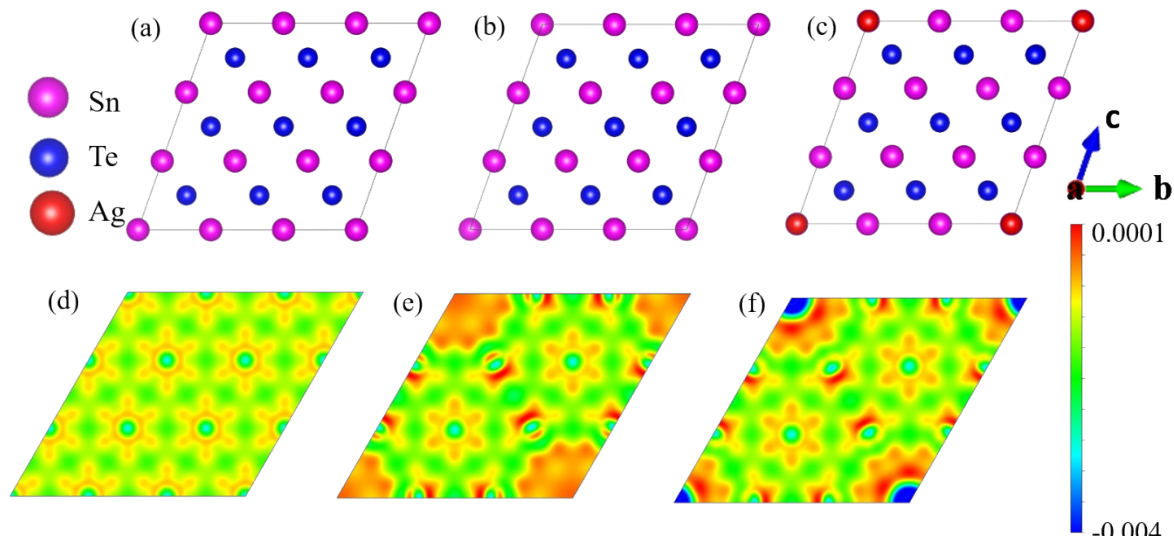


Fig. S1 Sn₂₇Te₂₇ (a), Sn₂₆Te₂₇ (b), and Sn₂₆AgTe₂₇ (c) primitive cells used for the DFT calculations, and the 2-dimensional charge density difference for the (001) planes of Sn₂₇Te₂₇ (d), Sn₂₆Te₂₇ (e), and Sn₂₆AgTe₂₇(f). Blue and yellow colours represent loss and gain of electrons, respectively.

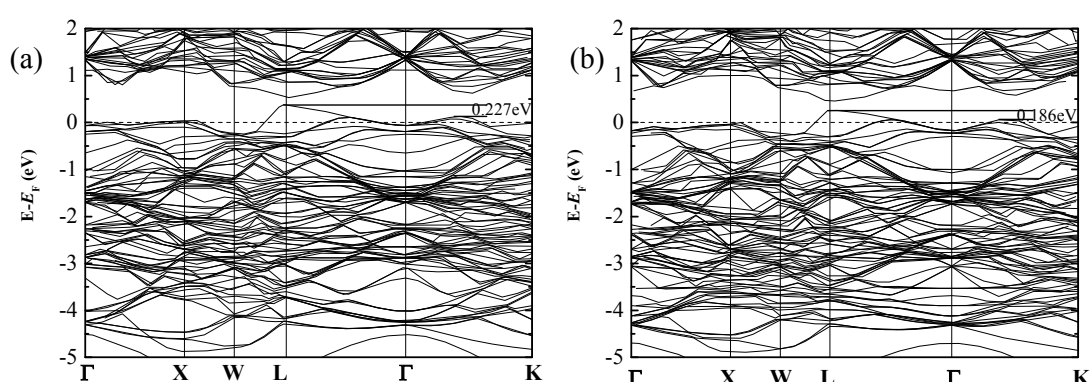


Fig. S2 Calculated electronic band structures for the Sn-deficient Sn₂₆Te₂₇ (a) and silver-doped Sn₂₆AgTe₂₇ (b) using Perdue Burke Ernzerhof generalized gradient approximations (PBE-GGA) based on density functional theory (DFT).

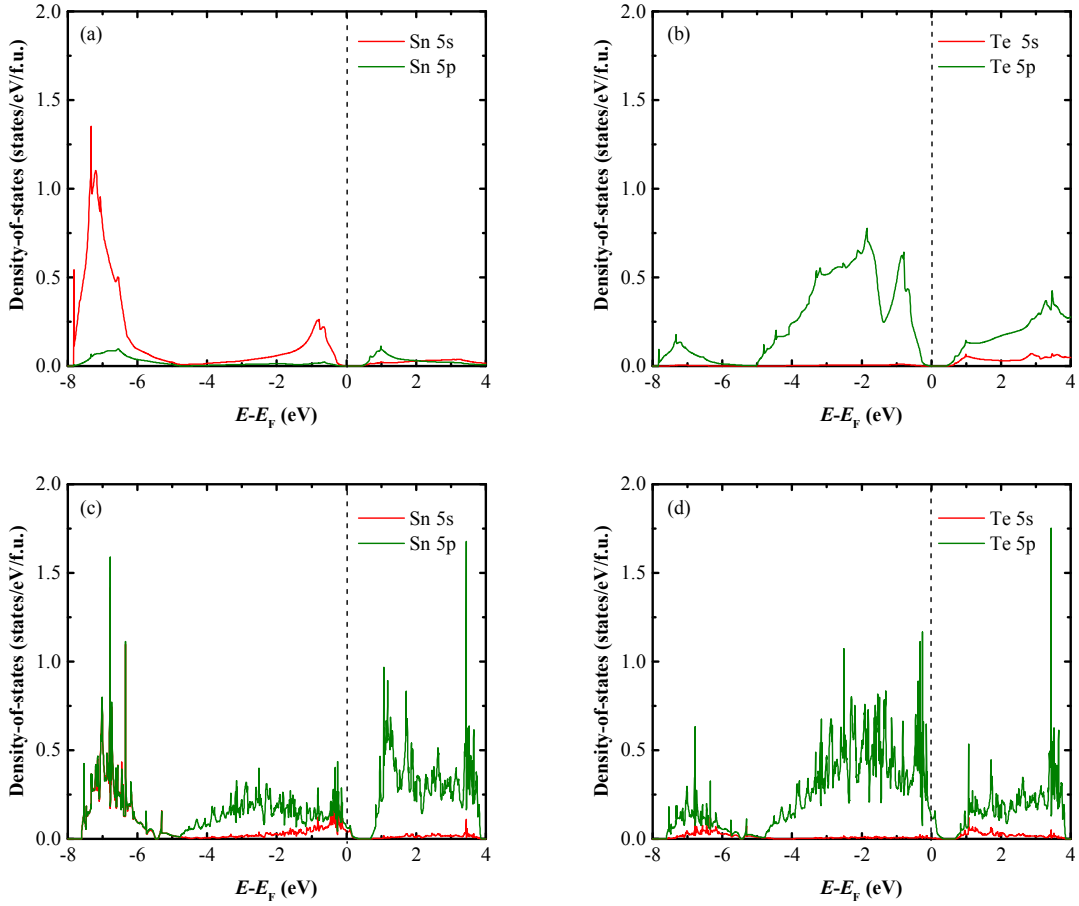


Fig. S3 Calculated partial electronic density-of-states (DOS) for SnTe (a, b) and $\text{Sn}_{26}\text{Te}_{27}$ (c, d) based on the DFT method.

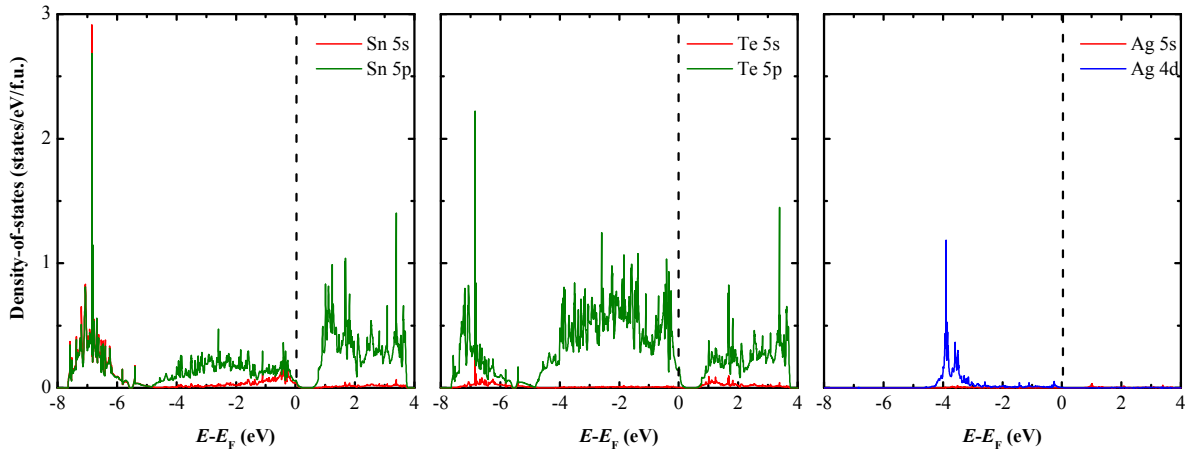


Fig. S4 Calculated partial electronic density-of-states (DOS) for the silver doped $\text{Sn}_{26}\text{Ag}\text{Te}_{27}$ based on the DFT method.

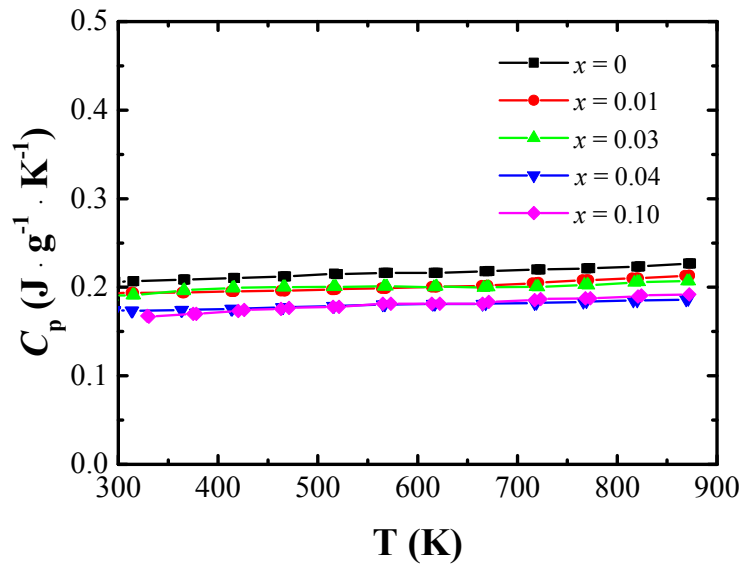


Fig. S5 Temperature dependence of the specific heat for the excess-silver-doped SnAg_xTe ($x = 0, 0.01, 0.03, 0.04, 0.10$) samples.

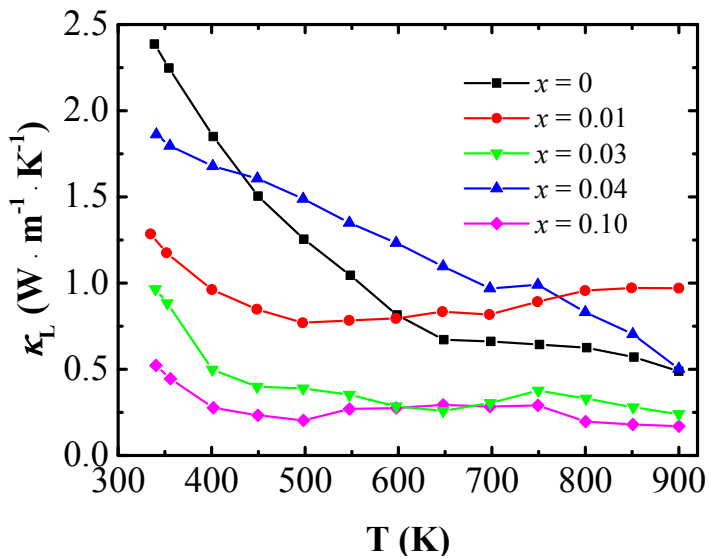


Fig. S6 Temperature dependence of the lattice thermal conductivity (κ_L) for the synthesized SnAg_xTe ($x = 0, 0.01, 0.03, 0.04, 0.10$) samples.